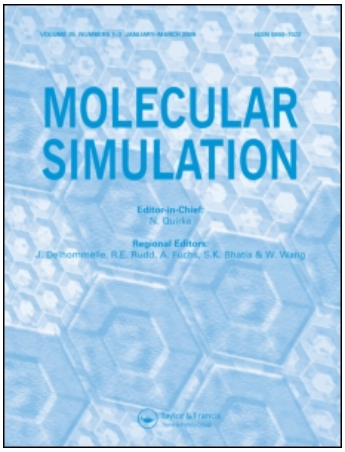


**Molecular Simulation**
Publication details, including instructions for authors and subscription information:
http://www.informaworld.com/smpp/title~content=t713644482

# Microphase separation of graft-diblock copolymer by dissipative particle dynamics simulation

Yi Xu[a]; Jian Feng[a]; Honglai Liu[a]; Ying Hu[a]
[a] Laboratory for Advanced Material, East China University of Science and Technology, Shanghai, P. R. China

**To cite this Article** Xu, Yi , Feng, Jian , Liu, Honglai and Hu, Ying(2008) 'Microphase separation of graft-diblock copolymer by dissipative particle dynamics simulation', Molecular Simulation, 34: 5, 559 — 565
**To link to this Article: DOI:** 10.1080/08927020801930570
**URL:** http://dx.doi.org/10.1080/08927020801930570

*Molecular Simulation*
Vol. 34, No. 5, April 2008, 559–565

Taylor & Francis
Taylor & Francis Group

# Microphase separation of graft-diblock copolymer by dissipative particle dynamics simulation

Yi Xu[a,b,c], Jian Feng[a,b,d], Honglai Liu[a,b]* and Ying Hu[a,b]

[a]*Laboratory for Advanced Material, East China University of Science and Technology, Shanghai, P. R. China;* [b]*Department of Chemistry, East China University of Science and Technology, Shanghai, P. R. China;* [c]*Department of Chemical Engineering, Shanghai University, Shanghai, P. R. China;* [d]*Department of Chemistry, Chuzhou University, Chuzhou, Anhui, P. R. China*

(*Received 9 June 2007; final version received 19 January 2008*)

Microphase-separation behaviour of graft-diblock copolymers was investigated by the dissipative particle dynamics. Besides familiar totally ordered mesostructures, the simulated phase diagram also shows unfamiliar locally ordered mesostructures together with a few melted morphologies. The simulated order–disorder transition critical value is higher than the theoretically predicted value due mainly to the increasing fluctuation coming from finite chain length. The microphase-separation morphologies in graft-diblock copolymers shift away significantly from that of the corresponding linear ones with the same component volume fractions. Generally, it is more difficult to trigger microphase separation for graft-diblock copolymers than for their linear analogues, in good agreement with theoretical and experimental findings. The change of graft fraction has a significant effect on the microphase-separation behaviour of graft-diblock copolymers.

**Keywords:** microphase separation; graft-diblock copolymer; dissipative particle dynamics



## 1. Introduction

Block copolymers have received much attention over the past few decades due to their ability to form various ordered mesostructures depending on the chain composition, temperature and external fields. Unlike blends of homopolymers whose phase separation occurs on a macroscopic level with separate domains formed for each polymer, phase separation of block copolymers happens on a microscopic level because the different blocks are chemically linked. The resulting microphases exhibit classical morphologies, such as lamellas (LAM), rods, spheres, bicontinuous structures [1–2], leading to novel properties and wide applications [3–8]. Understanding the microphase-separation behaviour of block copolymers is significant for utilising them more effective and better.

Studies on linear diblock copolymers have made much progress as the topology is relatively simple. However, linear triblock copolymers and nonlinear block copolymers with unique architectures, such as star, branch, graft, cyclic and comb shapes, have attracted less attention. Earlier, the mean-field theory was adopted in the research of triblock [9], graft, and star [10] copolymers by Cruz et al. and of asymmetric [11] and symmetric [12] comb copolymers. Moreover, fluctuation corrections have been incorporated for triblock [13] and star copolymers [14]. In terms of computer simulation, the existing few studies [15–21] were mostly based on traditional Monte Carlo technique. Recently, by means of dissipative particle dynamics (DPD) method, Qian et al. [22] studied the microphase separation of cyclic diblock copolymer which was compared with previous work [17]. The authors have also investigated the dynamics of microphase separation in star-diblock copolymer melts [23]. It has been recognised that either cyclic or star architecture can make the microphase-separation behaviours of nonlinear diblock copolymers differ remarkably from those of corresponding linear ones. As for graft block copolymers, although the relevant syntheses [24–28] have been developed profoundly, related simulation studies, even on the simplest graft-diblock copolymer, are rare. It is valuable, therefore, to study the effect of the graft architecture on physical properties of graft-diblock copolymers.

In general, an AB graft-diblock molecule is constructed simply by a linear A chain as the backbone grafted with a linear B chain, schematically shown in Figure 1. It can also be regarded as a three-armed star copolymer with two A arms and one B arm, or just a 'Y' architecture copolymer, which is distinctly different from previously studied $(A)_4(B)_4$ star copolymer [23] in the numbers of A and B arms. The volume fraction of A monomer in the graft copolymer is denoted as $f_A$ and the fractional position along the A chain at which the B graft is chemically linked is denoted as $\tau$. When $\tau = 0$ or 1, the graft copolymer degenerates to a simple diblock copolymer. Cruz and Sanchez [10] have calculated the phase stability criteria and static structure factors by mean-field theory near the order–disorder transition (ODT) for this system. The results show that for a given $\tau$, the spinodal value $(\chi N)_{ODT}$ always reaches a minimum at $f_A = 0.5$; for $\tau = f_A = 0.5$, $(\chi N)_{ODT} = 13.5$, in which $\chi$ is the Flory–Huggins

*Corresponding author. Email: hlliu@ecust.edu.cn

ISSN 0892-7022 print/ISSN 1029-0435 online

DOI: 10.1080/08927020801930570
http://www.informaworld.com

Figure 1. Schematic representation of AB graft-diblock copolymer, where the real and broken lines denote the A and B components, respectively.

parameter characterising the interaction between A and B components and $N$ is the number of monomer units in an AB graft copolymer. In addition, the $(\chi N)_{\mathrm{ODT}}$ values for all $0 < \tau < 1$ are distinctly higher than that for $\tau = 0$ or 1 implying that it is more difficult to phase separate a graft-diblock copolymer than a corresponding linear one. Milner [29] has derived by the mean-field calculations a phase diagram revealing that when the volume fraction of B graft component is $f_{\mathrm{B}} = 2/3$ in an $A_2B$ graft-diblock copolymer, a flat preferred interfacial curvature occurs. The distinct absence of a preferred curvature for symmetric diblock architecture at $f_{\mathrm{B}} = 1/2$ indicates the shift of the centre of the phase diagram due to architecture alone. Hadjichristidis et al. [30] and Pochan et al. [31] have found through the SAXS and TEM techniques that observed morphologies of their samples of $A_2B$ graft copolymers shift away from what would be formed by linear diblock analogues with the same component volume fractions. Lu et al. [28] have observed in previously prepared PSf-*g*-P*t*BA copolymer that in bulk the P*t*BA domain shape changes from wormlike to cylindrical and to lamellar as its volume fraction increases, where the wormlike and cylindrical morphologies lack long-range order and the alternating P*t*BA and PSf lamellae are packed regularly. There are also some other theoretical [32,33] and experimental [34–36] studies on this system. The aim of this work is to make a comprehensive investigation on its microphase-separation behaviour by mesoscopic simulations.

## 2. Simulation method and model construction

The DPD method was first introduced by Hoogerbrugge and Koelman [37,38] and gradually improved by various authors [39,40]. It has been applied to a wide field and has proved to be a versatile simulation technique for complex fluids on the mesoscopic scale [43]. The elementary units in DPD are fluid elements or coarse-grained soft particles representing a small region of fluid that contains a group of molecules. The time evolution is governed by Newtonian equations of motion [40]. The interparticle interacting force $\mathbf{F}_i$ contains three parts; each of them is pairwise additive,

$$\mathbf{F}_i = \sum_{j \neq i} (\mathbf{F}_{ij}^{\mathrm{C}} + \mathbf{F}_{ij}^{\mathrm{D}} + \mathbf{F}_{ij}^{\mathrm{R}}), \tag{1}$$

where the conservative force $\mathbf{F}_{ij}^{\mathrm{C}}$ is a soft repulsive force acting along the line of centres, the dissipative force $\mathbf{F}_{ij}^{\mathrm{D}}$ and the random force $\mathbf{F}_{ij}^{\mathrm{R}}$ act as heat sink and source, respectively, to provide a thermostat for the whole system. Additionally, there is a certain relationship between $\mathbf{F}_{ij}^{\mathrm{D}}$ and $\mathbf{F}_{ij}^{\mathrm{R}}$ to satisfy the fluctuation–dissipation theorem, so that the system can ensure (angular) momentum conservation leading to an accurate description of hydrodynamics [44]. The DPD method can therefore produce a correct canonical (*NVT*) ensemble [39].

Many integration schemes [40,45–47] have been proposed during the past few years. Among them the modified velocity-Verlet integrator developed by Groot and Warren [40] has been proved relatively efficient [22] and has been most widely applied. We adopt it in this work:

$$\begin{aligned}
\mathbf{r}_i(t + \Delta t) &= \mathbf{r}_i(t) + \Delta t \mathbf{v}_i(t) + \frac{1}{2}(\Delta t)^2 f_i(t), \boldsymbol{v}_i(t + \Delta t) \\
&= \mathbf{v}_i(t) + \lambda \Delta t \mathbf{f}_i(t), \mathbf{f}_i(t + \Delta t) \\
&= \mathbf{f}_i(\mathbf{r}(t + \Delta t), \boldsymbol{v}(t + \Delta t)), \mathbf{v}_i(t + \Delta t) \\
&= v_i(t) + \frac{1}{2}\Delta t(\mathbf{f}_i(t) + \mathbf{f}_i(t + \Delta t)).
\end{aligned} \tag{2}$$

The graft-diblock copolymer in simulations is modelled according to the sketch demonstrated in Figure 1. As shown in Figure 2, a graft molecule is constructed by a $m$-particle linear free A chain grafted with a $n$-particle linear free B chain at a middle position on the A chain, expressed as $(A_m)g(B_n)$, and each graft molecule consists of 30 soft particles with the same diameter $r_{\mathrm{c}}$, thus $N = m + n = 30$. The soft particles in a chain are connecting one by one through the harmonic springs with a spring force $\mathbf{F}_{ij}^{\mathrm{S}} = \mathbf{C}\mathbf{r}_{ij}$. The initial linking bond lengths between the neighbouring particles are all set equal to unit length. In this work, we adopted a 3D simulation cell of size $30 \times 30 \times 30$ with periodic boundary conditions applied in all three directions, which was found to be sufficiently large to eliminate the finite size effect. The number density $\rho$ equals to 3 and the total number of particles in the system is 81,000, corresponding

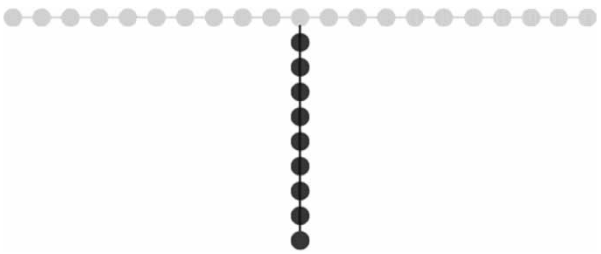

Figure 2. DPD model of graft-diblock copolymer. The grey and black particles represent the A and B blocks, respectively.

number of graft copolymers is 2700. Referring to literature work [22,41,42], we chose the relevant parameters as $k_BT = 1$, $\sigma = 3.67$, $\lambda = 0.65$, $\Delta t = 0.06$ and $C = 4$. For simplicity, the reduced temperature of the whole system in next sections is denoted as $T$.

For comparing with corresponding theoretical work [10], we focused mainly on how the composition of block A, $f_A$, and the energy parameter $\chi N$ influence the final mesoscopic ordered structures when the graft fraction is fixed at $\tau = 0.5$. Besides, the cases of other $\tau$ values have also been taken into account. For the $(A_m)g(B_n)$ copolymer, $f_A = m/(m+n)$. The Flory–Huggins $\chi$ parameter can be chosen appropriately within a certain range and transformed into the most important interaction parameter in DPD via the linear mapping relation established by Groot and Warren [40,41],

$$a_{ij} \approx a_{ii} + 3.27\chi_{ij} \quad (\rho = 3), \tag{3}$$

where $a_{ii}$ is the interacting energy between particles of the same type and in general $\alpha_{ii} = 25$.

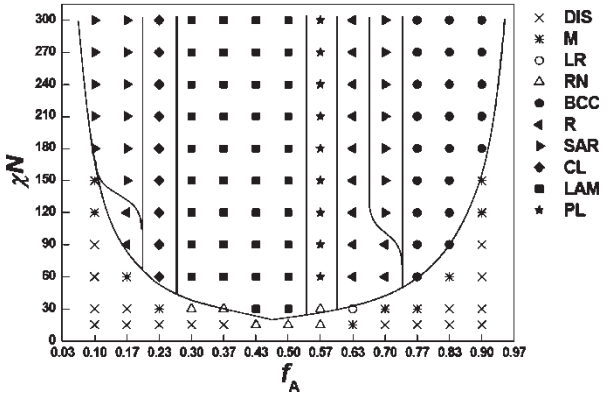


Figure 3. Simulated phase diagram for the graft-diblock copolymer at $\tau = 0.5$. Disordered phase (DIS), micelles (M), random network (RN), body-centred cubic spheres (BCC), rods (R), spheres and rods (SAR), connected lamellas (CL), lamellas (LAM) and perforated lamellas (PL) are displayed.

## 3. Simulation results and discussion

### *3.1 Phase diagram of the graft-diblock copolymer*

A series of mesoscopic structures have been obtained in the case of $\tau = 0.5$ through varying the composition $f_A$ and the A–B interaction parameter $\chi$. The phase diagram of graft copolymer with $\chi N$ as ordinate and $f_A$ as abscissa is shown in Figure 3. When the A–B interaction is relatively weak with smaller $\chi$, the system shows totally disordered state. As the interaction strengthens gradually, a sequence of transitions will occur. Several totally ordered structures that appeared in the microphase-separation behaviours of corresponding linear [48,49], cyclic [22,50] and star [10,23] diblock copolymers have been observed, such as LAM, perforated lamellas (PL) for symmetric or moderately symmetric cases in the composition and body-centred cubic spheres (BCC) for highly asymmetric cases, as shown in Figure 4. Besides, we have obtained some locally ordered structures in asymmetric regions, such as rods (R), spheres and rods (SAR), and connected LAM, depicted in Figure 5. Lu et al. [28] have found in their samples of graft-diblock copolymer a cylindrical morphology with only short-range order formed by the graft block of 30% in volume fraction, which is in accord with our simulated results both in the shape and composition. As far as we know, the other two morphologies have never appeared in previous relevant studies, thus they may be regarded as a complementary to them.

For macroscopic phase separation, generally, transition from one phase to another is a sudden change. For the micro-phase separation in this work, the simulated results show that there are some transition regions. For instance, the BCC has to transit through the SAR and R successively to the PL and subsequently to the LAM as $f_A$ varies at a fixed $\chi$. Furthermore, when $\chi$ increases gradually at a fixed $f_A$ the disordered phase has to pass by some melted morphologies to reach the totally ordered phases, such as micelles, liquid rods and random network. Similar phenomena have been identified in the DPD

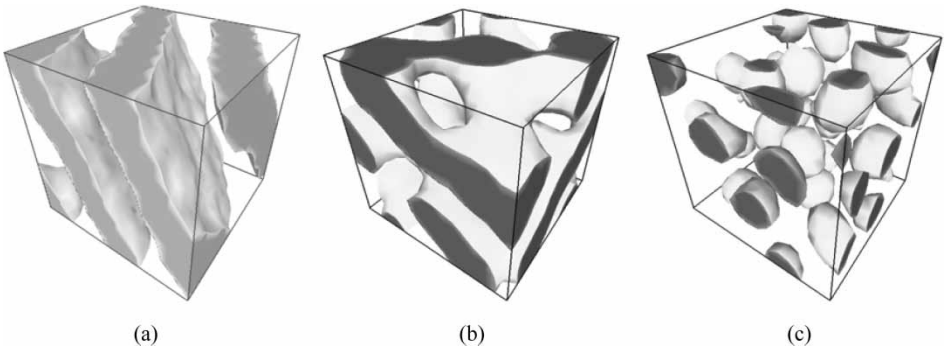


Figure 4. Several totally ordered structures formed in the graft-diblock copolymer melts. (a) LAM formed by $(A_{15})g(B_{15})$ at $\chi N = 210$; (b) PL formed by $(A_{17})g(B_{13})$ at $\chi N = 180$ and (c) BCC formed by $(A_{23})g(B_7)$ at $\chi N = 120$.

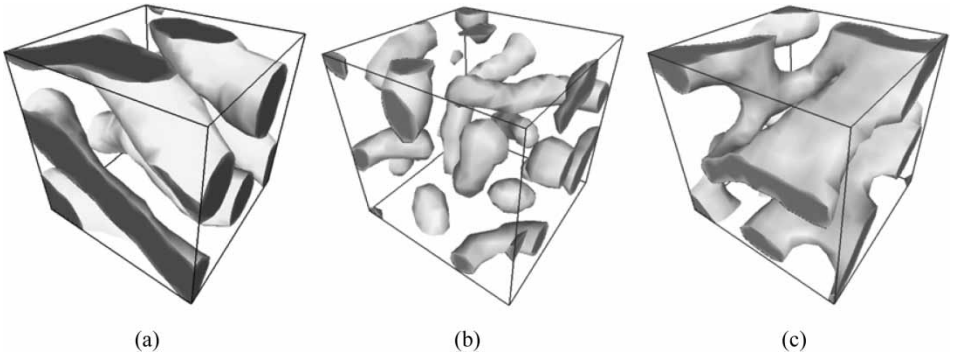


Figure 5. Several locally ordered structures formed in the graft-diblock copolymer melts. (a) R formed by $(A_{19})g(B_{11})$ at $\chi N = 300$; (b) SAR formed by $(A_5)g(B_{25})$ at $\chi N = 270$ and (c) CL formed by $(A_7)g(B_{23})$ at $\chi N = 300$.

simulations on the microphase-separation behaviours of linear [42], cyclic [22] and star [23] diblock copolymers. The morphologies of some melted phases, transition from disorder to order, are depicted in Figure 6.

### *3.2 Comparisons with the theoretical and experimental results*

The theoretical prediction [10] has told us the critical value $(\chi N)_{ODT}$ for graft-diblock copolymer of infinitely long Gaussian chain at $\tau = f_A = 0.5$ is 13.5, which is the minimum at this $\tau$. For locating accurately this value in our system, more simulation runs have been performed on the $(A_{13})g(B_{17})$ and $(A_{15})g(B_{15})$ (not displayed in Figure 3) showing the minimum of $(\chi N)_{ODT}$ exists in the $(A_{15})g(B_{15})$ and it is between 27.0 and 28.5. That is, the simulated threshold for the totally ordered phase to appear is higher than the theoretical prediction. This discrepancy has also been found in the DPD simulations on the microphase-separation behaviours of linear [41], cyclic [22] and star [23] diblock copolymers and can be ascribed basically to the increasing fluctuation with finite chain length adopted in the simulations, which lacks Gaussian statistics assumed generally in relevant theories. Weak coupling calculations [51] have shown that the ODT critical value for small linear diblock copolymers at $f = 0.5$ is $(\chi N)_{ODT} = 10.495 + 41.022N^{-[1/3]}$, following from which an expression has been put forward for relating the simulated $\chi N$ of the finite chain with that of the infinitely long chain from theoretical predictions [41], $(\chi N)_{infinite} = (\chi N)_{ODT}/(1 + 3.9N^{2/3-2\nu})$. Afterwards, this formula has been applied to prove the simulated ODT critical value for the symmetric case through a chain length mapping from cyclic diblock copolymers to corresponding linear ones [22]. Following this treatment, we can derive the ODT critical value for our graft-diblock copolymer at $\tau = f_A = 0.5$ and the calculated $(\chi N)_{ODT}$ is 23.3, which is closer to but still disagrees with our simulated result indicating that better analytic technique should be developed to interpret quantitatively the behaviour in the graft-diblock copolymer, especially for the asymmetric cases.

Theoretical [10,29] and experimental [30,31] studies have indicated that the microphase-separation behaviours of graft-diblock copolymers differ remarkably from those of corresponding linear ones. For the sake of detailed comparisons, we have simulated a phase diagram of linear diblock copolymer with a chain length of 30, as shown in Figure 7. Obviously, it is symmetric, while for graft-diblock copolymer the phase diagram is distinctly

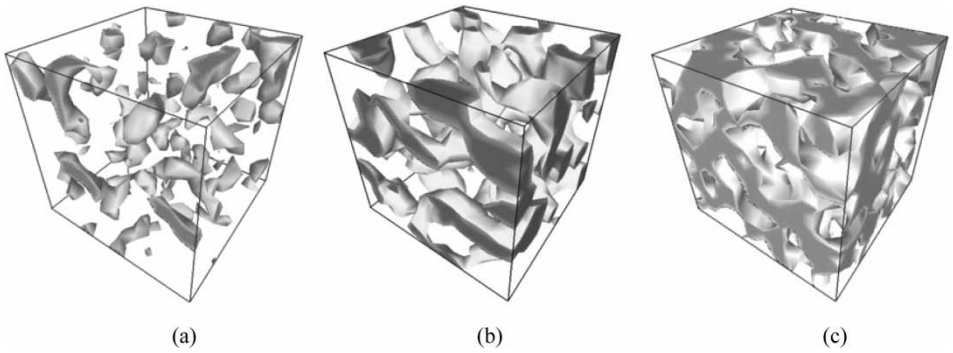


Figure 6. Several melted structures formed in the graft-diblock copolymer melts. (a) M formed by $(A_7)g(B_{23})$ at $\chi N = 30$; (b) LR formed by $(A_{19})g(B_{11})$ at $\chi N = 30$ and (c) RN formed by $(A_{15})g(B_{15})$ at $\chi N = 15$.

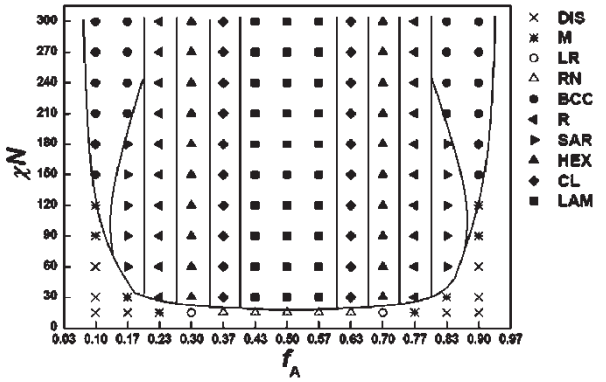


Figure 7. Simulated phase diagram for linear diblock copolymer with a chain length of 30. Disordered phase (DIS), micelles (M), liquid rods (LR), random network (RN), body-centred cubic spheres (BCC), rods (R), spheres and rods (SAR), hexagonal cylinders (HEX), connected lamellas (CL) and lamellas (LAM) are displayed.

asymmetric, consistent with the respective structural characteristic. The microphase-separation morphologies in graft-diblock copolymers deviate significantly from what would be formed by corresponding linear ones with the same component volume fractions, especially, the centre of LAM region has shifted away from the traditional $f_A = 0.5$, just as relevant theory and experiments disclosed [29–31]. As we all know, the microphase-separation structures formed in diblock copolymers are determined by a competition between the two blocks. Both of the blocks would prefer to be on the convex side of a curved interface which can give them more available volume close to the interface for relaxing. The competition is governed by the relative degrees of polymerisation of the two blocks. If the two blocks have comparable monomer fractions, then the balanced competition would result in flat interfaces leading to the lamellar phase. If they are not comparable, curved interfaces would be formed in which the block with the larger monomer fraction relaxes on the convex side and the smaller block stretches on the concave side forming cylinders or spheres. As for the $A_2B$ graft-diblock copolymer, we can see from Figure 2 that the A block would like to reside on the convex side of a curved interface when its fraction is equal to that of the B block, for the two A branches stretch in different directions inducing more space possession. Therefore, the fraction of B block should be more than that in the linear analogue to produce an actual microphase-separation structure. Additionally, it is evident that the initial position of ordered structure (solid symbol) at each composition in Figure 3 is higher than that at the same composition in Figure 7, except for the cases of $f_A = 0.43$ and 0.50. Additional simulations have shown that for the graft $(A_{13})g(B_{17})$ and $(A_{15})g(B_{15})$ the thresholds for LAM to appear are $\chi N = 30.0$ and 28.5, respectively, while for their linear analogues, i.e. $A_{13}B_{17}$ and $A_{15}B_{15}$, they separately equal to $\chi N = 27.0$ and 25.5. Thus, it can be seen that the microphase separation should be more difficult for graft-diblock copolymers than for their linear diblock analogues to occur under the same conditions, which is in agreement with the prediction of mean-field theory and can be attributed to the difference in entropy changes [10].

### 3.3 *Influence of the graft fraction* $\tau$

The influence of the graft fraction $\tau$ on the microphase-separation behaviours of graft-diblock copolymers has attracted less attention and it is worth investigation. The changes of simulated mesostructures with $\tau$ in several typical graft-diblock copolymers at $\chi N = 180$ are listed in Table 1, in which $\tau$ is chosen discretely due to the limit of graft model in Figure 2. Apparently, each change trend is symmetric about $\tau = 0.5$, which can be ascribed to the structural characteristics of graft copolymers. As $\tau$ increases from 0.5 to 1.0, or decreases to 0, the microphase-separated structures originally belong to the graft-diblock copolymers will transit gradually to those of corresponding linear ones, which is more evident in the copolymers with a relatively long backbone chain. Some more ordered structures have appeared during these processes, such as hexagonal cylinders (HEX), bicontinuous helices (H) and connected rods (CR), displayed in Figure 8, where the H can be considered the transition phase from LAM to HEX, and the CR, from R to HEX. With regard to the ODT critical value, detailed simulations have revealed that as the graft fraction of $(A_{15})g(B_{15})$ varies from 0.500 to 0.071 or 0.928, the threshold of LAM

Table 1. Changes of simulated mesostructures with $\tau$ in several typical graft-diblock copolymers at $\chi N = 180$.

| Copolymers | | Graft fractions and simulated mesostructures | | | | | | | | |
|---|---|---|---|---|---|---|---|---|---|---|
| $(A_3)g(B_{27})$ | $\tau$ | | 0 | | | 0.500 | | | 1.000 | |
| | Phases | | BCC | | | SAR | | | BCC | |
| $(A_9)g(B_{21})$ | $\tau$ | 0 | 0.125 | 0.250 | 0.375 | 0.500 | 0.625 | 0.750 | 0.875 | 1.000 |
| | Phases | HEX | H | H | LAM | LAM | LAM | H | H | HEX |
| $(A_{21})g(B_9)$ | $\tau$ | 0 | 0.150 | 0.300 | 0.450 | 0.500 | 0.550 | 0.700 | 0.850 | 1.000 |
| | Phases | HEX | CR | R | SAR | SAR | SAR | R | CR | HEX |

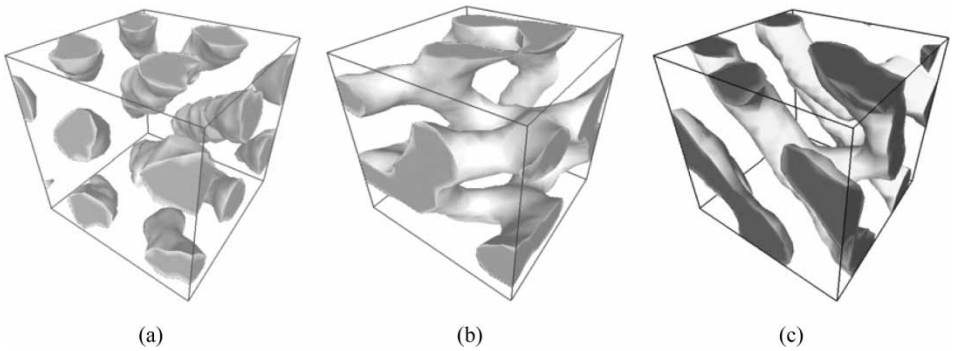


Figure 8. Several ordered structures formed in the graft-diblock copolymers in the case of $\chi N = 180$ and $\tau \neq 0.5$. (a) HEX formed by $(A_9)g(B_{21})$ at $\tau = 0$, i.e. $A_9B_{21}$; (b) H formed by $(A_9)g(B_{21})$ at $\tau = 0.125$ and (c) CR formed by $(A_{21})g(B_9)$ at $\tau = 0.150$.

decreases gradually from $\chi N = 28.5$ to 25.5, just equal to that of linear $A_{15}B_{15}$, for a graft-diblock copolymer will degenerate to its linear analogue when $\tau = 0$ or 1. Thus it can be seen that the change of graft fraction should have a significant influence on the microphase-separation behaviours of graft-diblock copolymer.

## 4. Conclusions

The microphase-separation behaviours of graft-diblock copolymers have been simulated by means of the DPD method. The simulated phase diagram shows several familiar totally ordered mesostructures together with some unfamiliar locally ordered structures and a few melted morphologies. The simulated ODT critical value obtained by simulation is higher than the theoretical prediction, which can be attributed to the increase of fluctuation originated from the finite chain length.

The microphase-separation morphologies in graft-diblock copolymers deviate significantly from what would be formed by corresponding linear ones with the same component volume fractions. Generally, it is more difficult for graft-diblock copolymers than for their linear analogues to trigger microphase separation. These findings are in accordance with the results from theoretical and experimental investigations. As the graft fraction increases or decreases from 0.5, the microphase-separation structures originally belong to the graft-diblock copolymers will transit gradually to those of corresponding linear ones indicating that the change of graft fraction has a significant influence on the microphase-separation behaviours of graft-diblock copolymer.

## Acknowledgements

This work is supported by the National Natural Science Foundation of China (No. 20606010, 20736002), the 111 Project of Ministry of Education of China (No. B08021), E-institute of Shanghai High Institution Grid (No. 200303) and Shanghai Municipal Education Commission of China.

## References

[1] F.S. Bates and G.H. Frederickson, *Block copolymer thermodynamics – theory and experiment*, Annu. Rev. Phys. Chem. 41 (1990), p. 525.
[2] F. Corberi, G. Gonnella, and A. Lamura, *Two-scale competition in phase separation with shear*, Phys. Rev. Lett. 83 (1999), p. 4057.
[3] W.A. Lopes and H.M. Jaeger, *Hierarchical self-assembly of metal nanostructures on diblock copolymer scaffolds*, Nature (Lond.) 414 (2001), p. 735.
[4] M. Templin, A. Franck, A. DuChesne, H. Leist, Y.M. Zhang, R. Ulrich, V. Schadler, and U. Wiesner, *Organically modified aluminosilicate mesostructures from block copolymer phases*, Science 278 (1997), p. 1795.
[5] L. Podariu and A. Chakrabarti, *Block copolymer thin films on corrugated substrates*, J. Chem. Phys. 113 (2000), p. 6423.
[6] T. Turn-Albrecht, J. Schotter, G.A. Kaestle, N. Emley, T. Shibauchi, L. Krusin-Elbaum, K. Guarini, C.T. Black, M.T. Tuominen, and T.P. Russell, *Ultrahigh-density nanowire arrays grown in self-assembled diblock copolymer templates*, Science 290 (2000), p. 2126.
[7] M. Park, C. Harrison, P.M. Chaikin, R.A. Register, and D.H. Adamson, *Block copolymer lithography: Periodic arrays of ~10 to the 11th power holes in 1 square centimeter*, Science 276 (1997), p. 1401.
[8] I.W. Hamley, *Nanostructure fabrication using block copolymers*, Nanotechnology 14 (2003), p. R39.
[9] A.M. Mayes and M. Olvera de la Cruz, *Microphase separation in multiblock copolymer melts*, J. Chem. Phys. 91 (1989), p. 7228.
[10] M. Olvera de la Cruz, *Theory of microphase separation in graft and star copolymers*, Macromolecules 19 (1986), p. 2501.
[11] H. Benoit and G. Hadziioannou, *Scattering theory and properties of block copolymers with various architectures in the homogeneous bulk state*, Macromolecules 21 (1988), p. 1449.
[12] A. Shinozaki, G. Jasnow, and A.C. Balazs, *Microphase separation in comb copolymers*, Macromolecules 27 (1994), p. 2496.
[13] A.M. Mayes and M. Olvera de la Cruz, *Concentration fluctuation effects on disorder–order transitions in block copolymer melts*, J. Chem. Phys. 95 (1991), p. 4670.
[14] A.V. Dobrynin and I. Ya. Erukhimovich, *Computer-aided comparative investigation of architecture influence on block copolymer phase diagrams*, Macromolecules 26 (1993), p. 276.
[15] A. Weyersberg and T.A. Vilgis, *Microphase separation in topologically constrained ring copolymers*, Phys. Rev. E. 49 (1994), p. 3097.
[16] G. Floudas, S. Pispas, N. Hadjichristidis, T. Pakula, and I. Erukhimovich, *Microphase separation in star block copolymers of styrene and isoprene: Theory, experiment, and simulation*, Macromolecules 29 (1996), p. 4142.
[17] W.H. Jo and S.S. Jang, *Monte carlo simulation of the order–disorder transition of a symmetric cyclic diblock copolymer system*, J. Chem. Phys. 111 (1999), p. 1712.

[18] V.V. Vasilevskaya, A.A. Klochkov, P.G. Khalatur, A.R. Khokhlov, and G. ten Brinke, *Microphase separation within a comb copolymer with attractive side chains: A computer simulation study*, Macromol. Theory Simul. 10 (2001), p. 389.
[19] T. Gemma, A. Hatano, and T. Dotera, *Monte Carlo simulations of the morphology of ABC star polymers using the diagonal bond method*, Macromolecules 35 (2002), p. 3225.
[20] J. Feng and E. Ruckenstein, *The morphology of symmetric triblock copolymer melts confined in a slit: A Monte Carlo simulation*, Macromol. Theor. Simul. 11 (2002), p. 630.
[21] ———, *Monte Carlo simulation of triblock copolymer thin films*, Polymer 43 (2002), p. 5775.
[22] H.J. Qian, Z.Y. Lu, L.J. Chen, Z.S. Li, and C.C. Sun, *Computer simulation of cyclic block copolymer microphase separation*, Macromolecules 38 (2005), p. 1395.
[23] Y. Xu, J. Feng, H. Liu, and Y. Hu, *Microphase separation of star-diblock copolymer melts studied by dissipative particle dynamics simulation*, Mol. Simul. 32 (2006), p. 375.
[24] G. Wang, Y. Shi, Z. Fu, W. Yang, Q. Huang, and Y. Zhang, *Controlled synthesis of poly(e-caprolactone)*-graft-*polystyrene by atom transfer radical polymerization with poly(e-caprolactone*-co-*a-bromo-e-caprolactone) copolymer as macroinitiator*, Polymer 46 (2005), p. 10601.
[25] L. Caporaso, N. Iudici, and L. Oliva, *Synthesis of well-defined polypropylene*-graft-*polystyrene and relationship between structure and the ability to compatibilize the polymeric blends*, Macromolecules 38 (2005), p. 4894.
[26] Y. Wu, Y. Zheng, W. Yang, C. Wang, J. Hu, and S. Fu, *Synthesis and characterization of a novel amphiphilic chitosan–polylactide graft copolymer*, Carbohydr. Polym. 59 (2005), p. 165.
[27] Y. Lu, S. Chen, Y. Hu, and T.C. Chung, *Synthesis of graft copolymer polyethylene*-graft-*poly(ethylene oxide) by a new anionic graft-from polymerization*, Polym. Int. 53 (2004), p. 1963.
[28] Z. Lu, G. Liu, and S. Duncan, *Polysulfone*-graft-*poly(*tert-*butyl acrylate): Synthesis, nanophase separation, poly(*tert-*butyl acrylate) hydrolysis, and pH-dependent iridescence*, Macromolecules 37 (2004), p. 174.
[29] S.T. Milner, *Chain architecture and asymmetry in copolymer microphases*, Macromolecules 27 (1994), p. 2333.
[30] N. Hadjichristidis, H. Iatrou, S.K. Behal, J.J. Chludzinski, M.M. Disko, R.T. Garner, K.S. Liang, D.J. Lohse, and S.T. Milner, *Morphology and miscibility of miktoarm styrene–diene copolymers and terpolymers*, Macromolecules 26 (1993), p. 5812.
[31] D.J. Pochan, S.P. Gido, S. Pispas, J.W. Mays, A.J. Ryan, J.P.A. Fairclough, I.W. Hamley, and N.J. Terrill, *Morphologies of microphase-separated A2B simple graft copolymers*, Macromolecules 29 (1996), p. 5091.
[32] G. Floudas, N. Hadjichristidis, H. Iatrou, T. Pakula, and E.W. Fischer, *Microphase separation in model 3-miktoarmStar copolymers (simple graft and terpolymers). 1. Statics and kinetics*, Macromolecules 27 (1994), p. 7735.
[33] G. Floudas, N. Hadjichristidis, H. Iatrou, and T. Pakula, *Microphase separation in model 3-miktoarm star co- and terpolymers. 2. dynamics*, Macromolecules 29 (1996), p. 3139.
[34] T. Miyata, T. Takagi, and T. Uragami, *Microphase separation in graft copolymer membranes with pendant oligodimethylsiloxanes and their permselectivity for aqueous ethanol solutions*, Macromolecules 29 (1996), p. 7787.
[35] C. Biver, G. de Crevoisier, S. Girault, A. Mourran, R. Pirri, J.C. Razet, and L. Leibler, *Microphase separation and wetting properties of palmitate*-graft-*poly(vinyl alcohol) films*, Macromolecules 35 (2002), p. 2552.
[36] C. Gao, H. Möhwald, and J. Shen, *Thermosensitive poly(allylamine)*-g-*poly(*N-*isopropylacryl amide): Synthesis, phase separation and particle formation*, Thermosensitive 46 (2005), p. 4088.
[37] P.J. Hoogerbrugge and J.M.V.A. Koelman, *Simulating microscopic hydrodynamic phenomena with dissipative particle dynamics*, Europhys. Lett. 19 (1992), p. 155.
[38] J.M.V.A. Koelman and P.J. Hoogerbrugge, *Dynamic simulations of hard-sphere suspensions under steady shear*, Europhys. Lett. 21 (1993), p. 363.
[39] P. Español and P.B. Warren, *Statistical mechanics of dissipative particle dynamics*, Europhys. Lett. 30 (1995), p. 191.
[40] R.D. Groot and P.B. Warren, *Dissipative particle dynamics: Bridging the gap between atomistic and mesoscopic simulation*, J. Chem. Phys. 107 (1997), p. 4423.
[41] R.D. Groot and T.J. Madden, *Dynamic simulation of diblock copolymer microphase separation*, J. Chem. Phys. 108 (1998), p. 8713.
[42] R.D. Groot, T.J. Madden, and D.J. Tildesley, *On the role of hydrodynamic interactions in block copolymer microphase separation*, J. Chem. Phys. 110 (1999), p. 9739.
[43] S.L. Yuan, Z.T. Cai, and G.Y. Xu, *Mesoscopic simulation of aggregates in surfactant/oil/water systems*, Chin. J. Chem. 21 (2003), p. 112.
[44] P. Español, *Hydrodynamics from dissipative particle dynamics*, Phys. Rev. E. 52 (1995), p. 1734.
[45] G. Besold, I. Vattulainen, M. Karttunen, and J.M. Polson, *Towards better integrators for dissipative particle dynamics simulations*, Phys. Rev. E. 62 (2000), p. R7611.
[46] I. Vattulainen, M. Karttunen, G. Besold, and J.M. Polson, *Integration schemes for dissipative particle dynamics simulations: From softly interacting systems towards hybrid models*, J. Chem. Phys. 116 (2002), p. 3967.
[47] T. Shardlow, *Splitting for dissipative particle dynamics*, SIAM J. Sci. Comput. 24 (2003), p. 1267.
[48] L. Leibler, *Theory of microphase separation in block copolymers*, Macromolecules 13 (1980), p. 1602.
[49] A.J. Schultz, C.K. Hall, and J. Genzer, *Computer simulation of copolymer phase behavior*, J. Chem. Phys. 117 (2002), p. 10329.
[50] A.N. Morozov and J.G.E.M. Fraaije, *Phase behavior of ring diblock copolymer melt in equilibrium and under shear*, Macromolecules 34 (2001), p. 1526.
[51] G.H. Fredrickson and E. Helfand, *Fluctuation effects in the theory of microphase separation in block copolymers*, J. Chem. Phys. 87 (1987), p. 697.